The Random Material Point Method

Wang, Bin; Vardon, Phil; Hicks, Michael

Publication date
2017

Document Version
Accepted author manuscript

Published in
6th international symposium on geotechnical safety and risk

Citation (APA)
Wang, B., Vardon, P., & Hicks, M. (2017). The Random Material Point Method. In *6th international symposium on geotechnical safety and risk: Geo-Risk 2017* (pp. 460 - 466)
http://10.1061/9780784480717.044

The Random Material Point Method

Bin Wang,[1] Philip J. Vardon,[1] and Michael A. Hicks[1]

[1]Geo-Engineering Section, Department of Geoscience and Engineering, Delft University of Technology, P.O. Box 5048, 2600 GA, Delft, Netherlands.
e-mails: B.Wang@tudelft.nl; P.J.Vardon@tudelft.nl; M.A.Hicks@tudelft.nl

ABSTRACT

The material point method is a finite element variant which allows the material, represented by a point-wise discretization, to move through the background mesh. This means that large deformations, such as those observed post slope failure, can be computed. By coupling this material level discretization to the spatial variability of the material generated by random fields and embedding this into a Monte Carlo framework, a new method called the Random Material Point Method (RMPM) has been developed. This method retains the advantages of the so-called random finite element method, that is, a risk based interpretation of the influence of spatial variability of the material properties, but additionally enables the effective modeling of large deformations to give a risk based interpretation of post-failure mechanisms. After a brief introduction to the RMPM methodology, the analysis of an idealized cohesion strain-softening clay slope is presented, which illustrates the influence of anisotropy of the material variability on the evolution of retrogressive slope failures.

INTRODUCTION

Soils exhibit substantial spatial variability, which has been more recently included in geotechnical analyses, for example, using the random finite element method, RFEM (e.g. Hicks and Samy 2002; Fenton and Griffiths 2008). Additionally, soil failures often involve large deformations which are typically unsuitable for simulations using static mesh-based methods such as the finite element method. The material point method (MPM) was proposed by Sulsky et al. (1994) to tackle large deformations and has been recently used in geotechnical simulations (e.g. Wang et al. 2016b,c), to model the entire slope failure process, from initiation to the development of multiple failures and the final failed configuration.

This paper presents a recent development, where the spatial variability and large deformations are captured in a method called the random material point method (RMPM) (Wang et al., 2016a). In this method, the spatial variability is captured by the generation of random fields and the large deformations are modeled by the material point method. This development sits alongside further developments in RFEM, which can also be used in conjunction with

RMPM, such as reducing uncertainties by including measured data (Vardon et al. 2016; Li et al. 2016), detecting scales of fluctuation in practice (Lloret-Cabot et al. 2014; de Gast et al. 2017), and efficiently dealing with low computed probabilities (van den Eijnden et al. 2017). It is seen that methods such as RFEM and RMPM, while computationally intensive, offer greater accuracy and flexibility than simpler methods utilizing probabilistic methods (Li et al. 2015; Varkey et al. 2017).

THEORETICAL BASIS

The material point method uses the same spatial discretization and, therefore, solution methods, as the finite element method (FEM). The major differences are that, in contrast to FEM, numerical integration (e.g. to form the mass matrix) and state variables (e.g. velocity and position, in this case) are associated with the material points rather than Gauss points, and that the mesh is reset after each solution step. This involves mapping between the material points and mesh nodes, and vice versa, at the beginning and end of the solution step, respectively.

Figure 1 shows the main stages of the computational procedure. In Figure 1(a), state variables are mapped to an arbitrarily located mesh; in Figure 1(b), a FEM calculation is undertaken to update the state variables on the mesh, with numerical integration undertaken via use of the material points; in Figure 1(c), the material point positions and state variables are updated. For the next step in the analysis the mesh is typically reset, although the mesh can be positioned differently, if required.

In this paper, the conservation of momentum is used as the governing equation and the equation is solved explicitly. In the work of Wang et al. (2016b,c), the equations were solved implicitly, which offers advantages with respect to the time step size. However, due to the wide range of material parameter values and plastic behaviors modeled in an RMPM analysis, it was decided to use the explicit version here. More details of the respective formulations are given by Wang et al. (2016a,b,c).

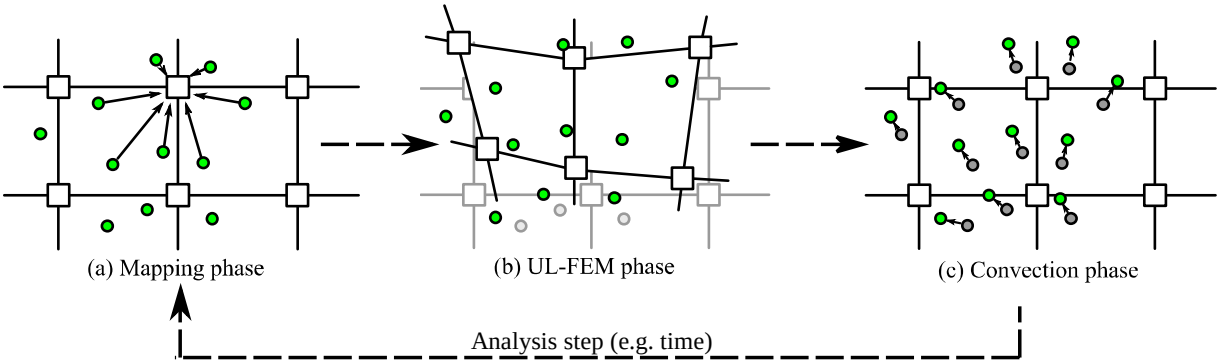

Figure 1. The stages of the material point method (after Wang et al. 2016a).

Random field theory allows the numerical generation of possible property fields, or realizations, based upon a statistical description of the field (Fenton and Griffiths, 2008). The required statistics are the point statistics of a probability density function, e.g. the mean and

standard deviation, and a description of the spatial correlation, e.g. a function characterized by the scale of fluctuation. Random fields are typically produced for a standard normal distribution and isotropic spatial correlation, and then transformed to the required statistical distribution and anisotropic properties.

The combination of random fields and FEM, called the random finite element method (RFEM), maps cell values from the random fields onto the Gauss points of an FEM mesh and each realization is then calculated deterministically (e.g. Hicks and Spencer 2010) in a Monte Carlo analysis. The main result of such an analysis is the quantification of the probability of any particular outcome, e.g. the stability of a slope.

RMPM maps values from the cells of the random fields to the material points, which, in this case, are located initially on the Gauss point locations of the background mesh. To quantify the range of possible responses, a Monte Carlo analysis is carried out (as in RFEM). However, this paper confines itself to illustrations (i.e. single realizations) of failure mechanism development, rather than to a quantification of risk. For more information on the Monte Carlo analysis technique and the quantification of slope-run out risk using RMPM, see Wang et al. (2016a).

ANALYSES

A simple slope analysis is presented to demonstrate the potential of RMPM in computing various failure mechanisms.

Domain and boundary conditions

A 5 m thick clay layer overlays a sloping bedrock, as shown in Figure 2. The main slope is 20° to the horizontal and, towards the bottom of the slope, a steeper slope (45° to the main slope surface) is cut. The upper-most section of the slope is horizontal. The domain is discretized into 4600 finite elements, with 4 material point initially placed in each element.

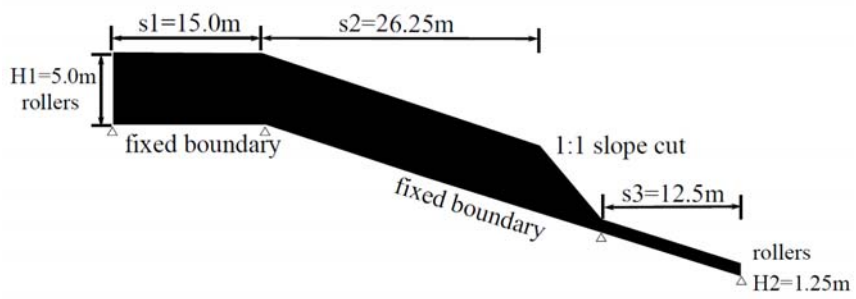

Figure 2. Domain and boundary conditions (not to scale).

Material properties

A simple linear elastic, cohesion softening model is used, with a Von Mises yield criterion. The Young's modulus and Poisson's ratio are 1000 kPa and 0.33, respectively, the soil self-weight is

20.0 kN/m^3, the mean peak cohesion is 20.0 kPa and the mean residual cohesion is 4.0 kPa. The coefficient of variation, i.e. the ratio between the standard deviation and mean, for both the peak and residual cohesion is 0.25. For each realization, a single random field of peak cohesion is generated, from which the random field of residual cohesion is back-figured, i.e. the peak and residual cohesion are proportional to each other. The material properties have been selected so that the slope is initially unstable, i.e. the slope instability is triggered by its self-weight.

Four case studies have been examined here: (i) a homogenous case, (ii) an isotropic spatial correlation, (iii) a mid-range anisotropic spatial correlation, and (iv) an extended anisotropic spatial correlation, where the appearance is almost layered. The vertical scale of fluctuation, θ_v, in cases (ii)-(iv) is 0.5 m, and the degree of anisotropy ($\xi = \theta_h / \theta_v$) for cases (ii), (iii) and (iv) are 1, 12 and 48, respectively. Single realizations of the peak cohesion for cases (ii)-(iv) are shown in Figure 3.

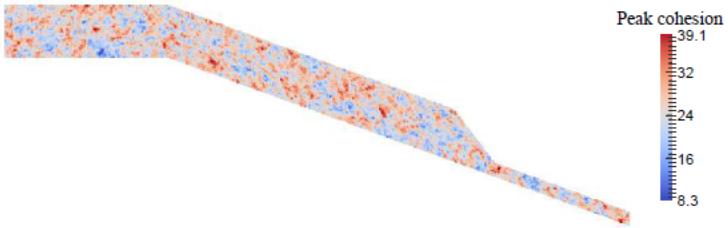

(a) ξ = 1, random field of peak cohesion (kPa)

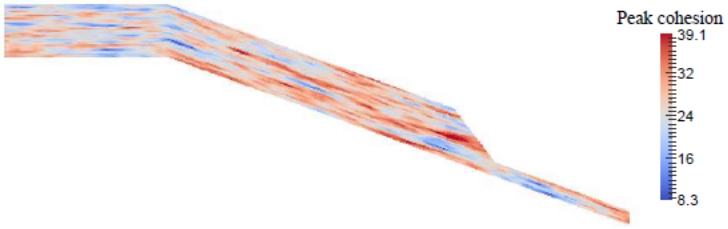

(b) ξ = 12, random field of peak cohesion (kPa)

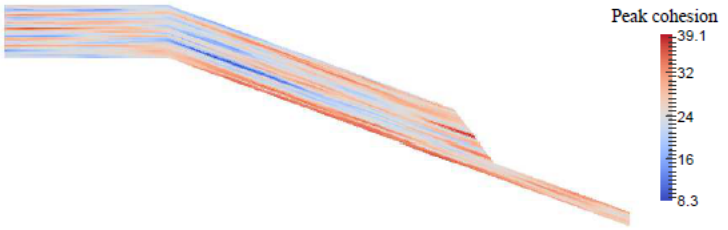

(c) ξ = 48, random field of peak cohesion (kPa)

Figure 3. Realizations of the peak cohesion for different anisotropies of the heterogeneity.

RESULTS

The result of the case (i) analysis is shown in Figure 4. As expected, and as would be predicted by an FEM analysis, the failure is a long translational slide along the base of the soil layer (as indicated by the high plastic shear strain invariant values). The MPM analysis also shows the subsequent breaking up of the slope mass as the deformation evolves into a succession of almost rotational slip planes.

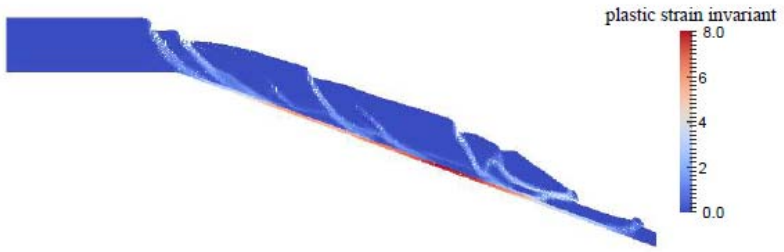

Figure 4. Plastic shear strain invariant contours for case (i): mean properties.

The results from cases (ii)-(iv) are shown in Figure 5(a)-(c). In Figure 5(a), there are only limited differences between the observed failure mechanism and that seen in Figure 4. The general failure mechanism is still that of a translational failure with the basal failure plane at the base of the soil layer. Similar sized and shaped sub-blocks are formed when the large sliding mass breaks up. A limited number of additional shear planes are seen moving away from the base and at the toe of the slope where weak zones are connected together.

For case (iv), where the highest level of anisotropy occurs, the material properties give the soil an almost layered appearance. This leads to a translational failure of the entire slope (see Figure 5(c)), though not at the base of the soil layer but at approximately one third of the depth from the base. The slope does not break up as much as in case (i), although some sub-blocks are formed at the top of the slope.

For the mid-range anisotropy, case (iii), shown in Figure 5(b) a more complex failure scenario is seen. A rotational failure is observed at the toe of the slope, and smaller rotational failures at the crest of the slope. A series of translational failures are also seen, interacting with each other. The material is observed to be the most disturbed of the three cases (i.e. it has the largest number of sub-blocks).

The differences in the observed failure mechanisms give rise to different amounts of material moving downslope, different early indications of slope failure and a range of outcomes, in contrast to the single outcome calculated in the homogenous case shown in Figure 4. Noting that each of the analyses presented here is statistically equal (with respect to the mean and standard deviation), the results suggest that, to quantify the risk associated with such slope failures requires knowledge of the uncertainty and spatial correlation of material parameters, in particular where the degree of anisotropy falls into the mid-range exemplified by case (iii).

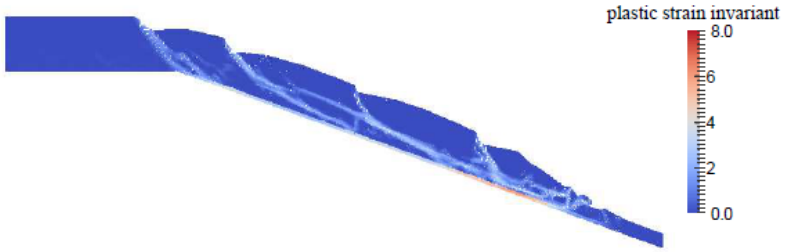

(a) ξ = 1, plastic shear strain invariant contours

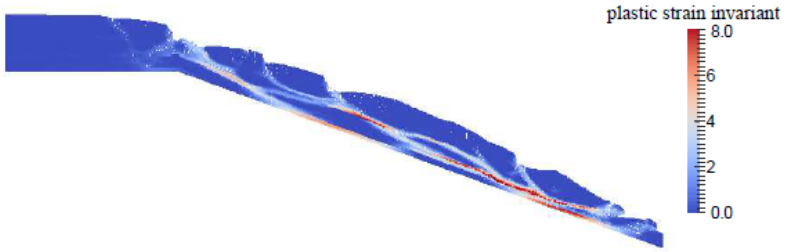

(b) ξ = 12, plastic shear strain invariant contours

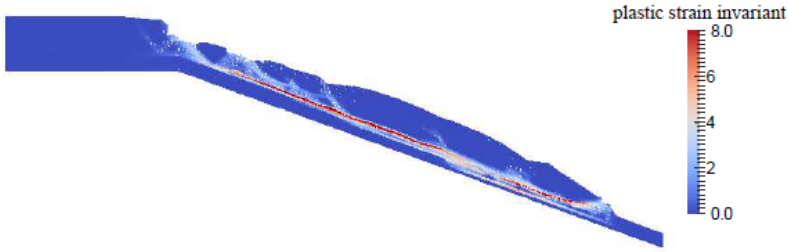

(c) ξ = 48, plastic shear strain invariant contours

Figure 5. Plastic shear strain invariant contours for cases (ii)-(iv): random realizations with different anisotropies of the heterogeneity.

CONCLUSION

The random material point method, a combination of random field theory and the material point method has been outlined. Example analyses, based on a long slope which typically would fail by translation, are shown, demonstrating the range of failure mechanisms observed. This method can be incorporated into a Monte Carlo analysis to quantify risk, based upon, for example, material sliding, or run-out length.

REFERENCES

Eijnden, B. van den, Hicks, M. A., and Vardon, P. J. (2017) "Investigating the influence of conditional simulation on small-probability failure events using subset simulation." *Accepted for ISGSR 2017.*

Fenton, G. A., and Griffiths, D. V. (2008). *Risk assessment in geotechnical engineering*. New York, NY, USA: John Wiley and Sons.

Gast, T. de, Vardon, P. J., and Hicks, M. A. (2017). "Estimating spatial correlations under man-made structures on soft soils." *Accepted for ISGSR 2017.*

Hicks, M. A., and Samy, K. (2002). "Influence of heterogeneity on undrained clay slope stability". *Q. J. Engng. Geol. Hydrogeol.,* 35(1), 41-49.

Hicks, M. A., and Spencer, W. A. (2010). "Influence of heterogeneity on the reliability and failure of a long 3D slope". *Comput. Geotech.*, 37(7-8), 948-955.

Li, Y. J., Hicks, M. A., and Nuttall, J. D. (2015). "Comparative analyses of slope reliability in 3D." *Engng. Geol.*, 196, 12-23.

Li, Y. J., Hicks, M. A., and Vardon, P. J. (2016). "Uncertainty reduction and sampling efficiency in slope designs using 3D conditional random fields." *Comput. Geotech.*, 79, 159-172.

Lloret-Cabot, M., Fenton, G. A., and Hicks, M. A. (2014). "On the estimation of scale of fluctuation in geostatistics." *Georisk: Assessment and Management of Risk for Engineered Systems and Geohazards*, 8(2), 129-140.

Sulsky, D., Chen, Z., and Schreyer, H. L. (1994). "A particle method for history-dependent materials." *Comput. Methods Appl. Mech. Engng.,* 118(1), 179-196.

Vardon, P. J., Liu, K., and Hicks, M. A. (2016). "Reduction of slope stability uncertainty based on hydraulic measurement via inverse analysis." *Georisk: Assessment and Management of Risk for Engineered Systems and Geohazards,*10(3), 223-240.

Varkey, D., Hicks, M. A., and Vardon, P. J. (2017). "Influence of spatial variability of shear strength parameters on 3D slope reliability and comparison of analysis methods." *Accepted for ISGSR.*

Wang, B., Hicks, M. A., and Vardon, P. J. (2016a). "Slope failure analysis using the random material point method." *Géotechnique Letters*, 6(2), 113-118.

Wang, B., Vardon, P. J., and Hicks, M. A. (2016b). "Investigation of retrogressive and progressive slope failure mechanisms using the material point method." *Comput. Geotech.*, 78, 88-98.

Wang, B., Vardon, P. J., Hicks, M. A., and Chen, Z. (2016c). "Development of an implicit material point method for geotechnical applications." *Comput. Geotech.*, 71, 159-167.